Taylor-Aris Disperson in High Aspect Ratio Columns of Nearly Rectangular Cross Section.

Michael L. Parks [1], Louis A. Romero [1,*]

Computational Mathematics and Algorithms, Sandia National Laboratories
P.O. Box 5800, MS 1320, Albuquerque NM 87185-1320

Abstract

We consider Taylor-Aris dispersion in columns of nearly rectangular cross section of large aspect ratio. We generalize the results of [1] and [2] who showed that the effective diffusion rate for perfectly rectangular cross sections is remarkably different than the diffusion rate between two parallel plates – as the aspect ratio goes to infinity, the effective diffusion rate does not approach the effective diffusion rate for two parallel plates. In particular, we examine columns of nearly rectangular cross section having both non-parallel walls and asymmetric ends of arbitrary shape. In particular, this includes geometries common to microfabricated gas chromatography columns. We develop an expression for the effective diffusivity showing the contributions from the walls and the ends, and the relative importance of each. We also discuss the large effect that a small nonuniformity in the middle of the cross section can have on the effective diffusion rate, and how the ends of the cross section can be modified to control the effective diffusion rate.

Key words: Taylor-Aris dispersion, gas chromatography, high aspect ratio, end effects

1 Introduction

In the classical papers by G. I. Taylor [3] and Rutherford Aris [4], they considered the advection and diffusion of a solute down a straight tube whose diameter is much smaller than its length. They showed that the solute is advected down the tube with the average

* Corresponding author.
Email addresses: mlparks@sandia.gov (Michael L. Parks), lromero@sandia.gov (Louis A. Romero).

[1] Sandia is a multiprogram laboratory operated by Sandia Corporation, a Lockheed-Martin Company, for the United States Department of Energy's National Nuclear Security Administration under contract DE-AC-94AL85000.

velocity of the fluid in the tube, and that its concentration profile satisfies a one dimensional advection diffusion equation with an effective diffusion constant that has the form

$$D_{eff} = D\left(1 + KPe^2\right). \tag{1}$$

Here D is the diffusivity of the solute, K is a constant that depends only on the geometry of the cross section of the tube, and Pe is the Péclet number

$$Pe = \frac{R\overline{u}}{D}.$$

Here R is the radius of the tube, and $\overline{u}$ is the average velocity of the fluid in the tube. One of the most striking features of this formula is that for large values of Pe, the effective diffusion coefficient is inversely proportional to the physical diffusivity. In [5], a similar analysis is used to lay the foundations for capillary gas chromatography.

In [2], Doshi, Daiyai, and Gill considered Taylor-Aris dispersion in rectangular cross sections of large aspect ratio and came up with a surprising result, which we now summarize. Suppose the rectangular cross section has height H_0, width W, and define the inverse aspect ratio as

$$\epsilon = \frac{H_0}{W}.$$

Consider two dimensional Taylor-Aris dispersion between two parallel plates. Intuitively, we might expect that the effective diffusion coefficient for a rectangular channel approaches the effective diffusion coefficient for the case of two parallel plates as the inverse aspect ratio approaches zero. These authors showed that this is not the case. In particular, the constant K in (1) is about 8 times bigger for a rectangular cross section of arbitrarily high aspect ratio as it is for two parallel plates. This phenomenon was discovered independently in [6] and applied to the case of dispersion by turbulent flow in [1].

In [7], Guelle, Cox, and Brenner discovered a related phenomenon. For a smoothly varying cross section that has a high aspect ratio (such as an elongated ellipse), the constant K in (1) is proportional to $1/\epsilon^2$. This is equivalent to saying that the appropriate Péclet number to use in (1) is the Péclet number based on the width of the cross section, not on the height. For example, if we take a rectangular cross section of large aspect ratio, and we inscribe an elongated ellipse in it, the constant K for the inscribed ellipse will be on the order of $1/\epsilon^2$ times larger than the constant for the rectangle. This phenomenon is also discussed in [8] and [9]. A similar phenomenon was noted by Golay [6], who pointed out that in a large aspect ratio channel, even a mild deviation from a rectangular geometry could drastically effect the constant K.

With the exception of the papers by Dutta and Leighton [10–12], the papers concerning Taylor-Aris dispersion in large aspect ratio channels can be grouped into two categories. The first deal with cross sections where the middle part of the cross section is not close to rectangular [9,7]. In this case the constant K is proportional to $1/\epsilon^2$, and any end effects will give only a small correction to this value. The other class of papers deal with the specific case of a rectangular cross section. The papers in this class [13–16] all are concerned with the effects of the ends. They discuss the end effect by doing asymptotics on the analytical expression (an infinite series expansion) for the constant K in a rectangular channel.

The purpose of this paper is to present an analysis of Taylor-Aris dispersion in nearly rectan-

gular cross sections of high aspect ratio. By nearly rectangular, we mean that the geometry of the walls of the middle of the cross section deviate only slightly from the rectangular case, but near the ends we may deviate significantly from a rectangular cross section. We do not assume the ends are symmetric. This particular geometry is important for microfabricated gas chromatographs, and hence we believe it deserves special attention. We will present theory combining the effects upon the dispersion of the geometry of the middle of the cross section with the effects of the ends of the cross section, and show the relative importance of each.

Our paper offers contributions that complement and extend the results in [10–12]. In [12], the authors consider situations similar to those discussed in this paper, but develop their analysis using heuristic arguments based on an analogy between the layer of slowly moving fluid at the ends of the channel and the thin layer of stagnant fluid in gas chromatography (see equations 14 and 15 in [12]). Although they showed considerable insight in writing down these equations, essentially without derivation, we instead develop our analysis in a more rigorous fashion without recourse to heuristic arguments. However, we also show in Appendix B that our results agree with theirs for the case of nearly rectangular cross sections, thus providing support for their conclusions. Additionally, our analysis drops their restriction that the end effects at both ends be the same.

In [10], Dutta and Leighton discuss nearly rectangular cross sections and present numerical results to demonstrate the effect of modifying the geometry at the ends of a rectangular cross section. In particular, they show that by suitably modifying the ends of a rectangular cross section it is possible to reduce the dispersion to the value for a parallel plate. In their example they have the ends of the tube bulge out as in figure 2(a). For a symmetrical cross section, in order to achieve the nearly parallel plate result it is necessary to have the average velocity in the channel be the same as the average velocity for the parallel plate case. One would suspect that this requires that the ends bulge out. Though this result seems intuitive, we feel that it merits a proof, which we show in §5.

We now discuss the source of the large effect that the end regions and small distortions of the middle region can have on the dispersion coefficient. Away from the ends of the cross section, the flow exponentially approaches plane Poiseuille flow. That is, we have $u(x, y) \to u^{pp}(y)$ for x away from the ends, where $u^{pp}(y)$ is the velocity profile for Poiseuille flow between two parallel plates. When we compute the average velocity $\overline{u}$ of the flow in the channel we find (see (22) in § 4) that

$$\overline{u} = \overline{U}^{pp} - \epsilon \overline{U}^{pp} \left(\alpha_L + \alpha_R\right) + \mathcal{O}(\epsilon^2).$$

Here $\overline{U}^{pp}$ is the average velocity for Poiseuille flow between two parallel plates, and α_L and α_R are constants that depend on the geometry of the left (L), and right (R) end regions, but not on ϵ.

Assuming the mid section of our cross section has parallel side walls, we will see that (see (35))

$$K = K^{pp} + \frac{\alpha_L^2 - \alpha_L \alpha_R + \alpha_R^2}{3} + \mathcal{O}(\epsilon).$$

Here $K^{pp} = \frac{1}{210}$ is the effective diffusion coefficient for Taylor-Aris dispersion between two infinite parallel plates. Note that the effect of the end regions does not vanish even in the limit as $\epsilon \to 0$. Since the quadratic form $\alpha_L^2 - \alpha_L \alpha_R + \alpha_R^2$ is positive definite, the only way we can make the end correction vanish is if both α_L and α_R are identically zero.

In §5 we show that the only way we can make α_L (or α_R) vanish is if the end bulges out so that the height in the end regions exceeds the height in the middle region (as in figure 2(a)), and also in [10]. In the case of a symmetrical cross section where $\alpha_L = \alpha_R$, this requires that the ends be modified such that the average velocity in the channel is the same as the average velocity between two parallel plates. One might be tempted to think that in the non-symmetrical case, the dispersion could also be reduced to the parallel plate value by having the average velocity in the cross section be the same as the average velocity for the parallel plate case (for example, by having only one of the ends bulge out, as in figure 2(b), while keeping the other end as in a rectangular cross section), but we show that we can reduce the dispersion to its parallel plate value only if both α_L and α_R vanish, and hence only if both ends bulge out.

In this paper we also analyze the case where the walls of the middle of the cross section have a small deviation from the parallel plate geometry. Although they do not consider this case specifically, the results in [7] and [9] suggest that mild deviations from the parallel plate geometry could significantly change the constant K. This is consistent with the comments made by Golay [6], although his discussion of this point was limited to the case where the walls have a constant slope, and his remarks were both exceedingly brief and confusing.

We consider the case where the height of the cross section varies as a function of x as

$$H(x) = H_0 \left(1 + \delta\gamma(x/W)\right).$$

In § 7 we show that assuming δ and ϵ are both small, we have

$$K \approx K^{pp} + \frac{\alpha_L^2 - \alpha_L\alpha_R + \alpha_R^2}{3} + K_1(\alpha_L, \alpha_R)\frac{\delta}{\epsilon} + K_2\frac{\delta^2}{\epsilon^2},$$

Here K_2 is independent of ϵ ,δ, α_L, and α_R. The constant $K_1(\alpha_L, \alpha_R)$ is independent of δ and ϵ, and is linear in α_L and α_R. This equation shows both the effects of the ends of the cross section, and the effects from variations in the middle of the cross section, and the relative effect caused by each. We see that even if δ and ϵ are both small we can in fact get a very large change in the effective diffusion constant due to a small variation in the cross section.

This work was largely motivated by problems in gas chromatography where microfabrication techniques have made it convenient to manufacture gas chromatography channels of nearly rectangular cross section. In this situation, we would like to keep K as small as possible. In particular, we show an end correction in § 8.2 that essentially recovers $K = K^{pp}$ for a column of rectangular cross section. The results given in this paper should be of immediate interest to the gas chromatography community.

We now summarize the contents of this paper. In § 2 we will discuss how to compute the effective diffusion coefficient for an arbitrary shaped cross section. Although this result is not entirely new, we believe that our formulation is simple enough that it deserves being written down, and is necessary for understanding the results for nearly rectangular cross sections. The derivation we give of how to compute K is similar to that given in [17] where the authors Fourier transform in the axial direction, but our results are applicable to any cross sectional shape, and our derivation is more succinct since we are only concerned with the long time behavior of the solution (e.g., the value of K).

In § 3 we compute the effective diffusion coefficient K^{pp} for flow between parallel plates. In § 4 we discuss how to compute the average velocity in a channel of nearly rectangular

cross section, which we will need for later sections. We see that the average velocity in a wide channel differs from the average velocity in an infinitely wide channel by an amount that is proportional to $\epsilon = H_0/W$. In § 5 we prove that in order to have α_L vanish, it is necessary to have the ends bulge out. In § 6 we give the results for mid-sections of constant height ($\delta = 0$), and in § 7 we give the results for slowly varying mid-sections ($\delta \neq 0$). In § 8, we confirm our results through direct numerical experiment. In Appendix A we give some details of the calculations that were omitted in the main part of the paper, and in Appendix B we compare our results to those in [12].

2 Taylor-Aris Dispersion for Arbitrarily Shaped Cross Sections

We consider the advection and diffusion of a solute down a column of constant but arbitrary cross section. We denote the cross section of the column by Ω, the boundary of the cross section by $\partial\Omega$, the area of the cross section as A, and the axial coordinate by z. The velocity down such a column is unidirectional and independent of z. In particular the velocity is given by $\underline{u} = (0, 0, u(x, y))$ where

$$\mu \nabla_2^2 u = \frac{\partial p}{\partial z} \text{ in } \Omega \tag{2a}$$

and

$$u = 0 \text{ on } \partial\Omega. \tag{2b}$$

Here ∇_2^2 represents the two dimensional Laplacian (ignoring the z component), μ is the dynamic viscosity of the fluid, and p is the pressure in the fluid.

Suppose a species with concentration $C(x, y, z, t)$ is being advected and diffused down the column. The evolution of the concentration distribution is given by [3]:

$$\frac{\partial C}{\partial t} + u(x, y)\frac{\partial C}{\partial z} = D\nabla^2 C, \tag{3a}$$

$$\frac{\partial C}{\partial n} = 0 \text{ on } \partial\Omega. \tag{3b}$$

The theory of Taylor-Aris dispersion shows that, assuming the length of the column is much greater than the characteristic length of the cross section, the evolution of the concentration profile is very well approximated by the one dimensional advection diffusion equation

$$\frac{\partial C}{\partial t} + \overline{u}\frac{\partial C}{\partial z} = D_{eff}\frac{\partial^2 C}{\partial z^2}. \tag{4}$$

Here $\overline{u}$ is the average value of the velocity, and D_{eff} is an effective diffusion constant that has the form given in (1). There have been numerous derivations of this result [4,14,18]. We give an alternative derivation that is an extension and simplification of the arguments used in [17].

Our derivation is based on the fact that the equations (3) are linear and invariant under arbitrary shifts in both t and z. The invariance under shifts in z make the equations amenable to an analysis by Fourier transforms. In particular, if $\hat{C}(x, y, k, t)$ is the Fourier transform in

z of $C(x,y,z,t)$, then for each value of k, $\hat{C}$ satisfies the evolution equation

$$\frac{\partial \hat{C}}{\partial t} + \mathrm{i}ku(x,y)\hat{C} = D\left(\nabla_2^2 \hat{C} - k^2 \hat{C}\right) \tag{5a}$$

along with

$$\frac{\partial \hat{C}}{\partial n} = 0 \text{ on } \partial\Omega. \tag{5b}$$

Due to the time shift invariance of these (and our original) equations, we can solve (5) by expanding $\hat{C}$ in terms of functions of the form $\exp\left(\sigma^{(m)}t\right)\ \phi^{(m)}(x,y,k)$, where $\sigma^{(m)}$ satisfies the eigenvalue problem

$$\sigma^{(m)}\phi^{(m)} + \mathrm{i}ku(x,y)\phi^{(m)} = D\left(\nabla_2^2 \phi^{(m)} - k^2\phi^{(m)}\right), \tag{6a}$$

$$\frac{\partial \phi^{(m)}}{\partial n} = 0 \text{ on } \partial\Omega. \tag{6b}$$

If $\sigma^{(m)}(k)$ is the m^{th} eigenvalue as a function of the wavenumber k, then for the $m = 0$ mode, this eigenvalue problem has the eigenvalue $\sigma^{(0)}(0) = 0$, along with the eigenfunction $\phi^{(0)}(0) = 1$. All of the other eigenvalues will be on the order of

$$\sigma^{(m)}(0) = \mathcal{O}(\frac{D}{R^2}), \quad m > 0,$$

where R is a characteristic length of the cross section. This shows that as long as $tD/R^2 > 1$, all of the modes with $m > 0$ will be rapidly damped out. Note that the time it takes for the concentration peak to move a distance l down the column is $t = 1/\overline{u}$. This means that the modes with $m > 0$ will be significantly damped out if $Pe\ R/l \ll 1$. Thus, as long as the Péclet number is not too large, and the length of the column is much greater than its characteristic diameter, we are justified in ignoring all but the mode $m = 0$. Physically this means that the profile will become nearly uniform across a cross section.

When $k \neq 0$, we get similar behavior. However, in this case the $m = 0$ mode will also be significantly damped if $tDk^2 \gg 1$. If as in the last paragraph we set $t = l/\overline{u}$, we see that any mode such that $R^2k^2 \gg Pe\ R/l$ will be significantly damped out. The main conclusion from all of this is that when analyzing the concentration profile down a long but very thin column, we need only concern ourselves with the small k limit of the mode $m = 0$. For ease of notation, we will refer to the eigenvalue of interest merely as $\sigma(k)$ (dropping the zero superscript). We will now use subscripts to denote the expansion of this eigenvalue in terms of a Taylor series in k. In particular if we write the expansion

$$\sigma(k) = \mathrm{i}\sigma_1 k + \sigma_2 k^2 + \ldots, \tag{7}$$

we can see that the one dimensional diffusion equation

$$\frac{\partial C}{\partial t} - \sigma_1 \frac{\partial C}{\partial z} = -\sigma_2 \frac{\partial^2 C}{\partial z^2}$$

satisfies the same dispersion relation as (4). That is, we have

$$\overline{u} = -\sigma_1 \qquad \text{and} \qquad D_{eff} = -\sigma_2.$$

A rigorous asymptotic analysis shows that as a solute is advected and diffused down a long narrow column, the concentration becomes nearly constant across a cross section, and the value of this concentration is governed by the above one dimensional advection diffusion equation. It should be noted that the above equation governs the long time behavior of the concentration profile. It does not, for example, resolve the fast initial transient that occurs if you place a species in the column with a nonuniform concentration distribution across the cross section of the column. Including higher order terms in (7) will lead to a one dimensional partial differential equation that has higher order spatial derivatives, and that is more accurate for shorter time scales. For a more complete discussion of the transient behavior in Poiseuille flow, see [17] and [19].

The above arguments show that the behavior of our solution can be well understood by determining the parameters σ_1 and σ_2. In this paper when we compute the Taylor-Aris dispersion coefficient numerically, we compute the eigenvalue $\sigma(k)$ for a few values of k that are small, and then do a polynomial curve fit of this function to determine σ_1 and σ_2. Alternatively, one can use the perturbation theory of eigenvalues to determine these quantities.

We omit the details, but the perturbation theory of eigenvalues shows that

$$\sigma_1 = -\overline{u}$$

and

$$\sigma_2 = -D - \frac{D}{A}\int_\Omega \mid \nabla\phi_1 \mid^2 \, \mathrm{d}A, \tag{8}$$

where $\overline{u}$ is the average value of the velocity, and ϕ_1 is the solution to

$$D\nabla_2^2\phi_1 = \left(u(x,y) - \overline{u}\right), \tag{9a}$$

$$\frac{\partial\phi_1}{\partial n} = 0 \text{ on } \partial\Omega. \tag{9b}$$

This solution is uniquely determined up to a constant, which does not influence the value of σ_2.

This is the expression for σ_2 that will be used in our analysis of rectangular and nearly rectangular cross sections. From (9) it should be clear that ϕ_1 is proportional to $\frac{\overline{u}}{D}$. The form of the above expression for σ_2 shows that when we put our equations in dimensionless form, the effective diffusion coefficient has the form described in (1).

3 Taylor-Aris Dispersion Between Two Parallel Plates

If our cross section is a rectangle with a very large aspect ratio, we might expect that the effective diffusion constant would be nearly equal to that calculated for the case of dispersion between two infinitely large flat plates. In the next few sections we will see that this is in fact not the case. As a preliminary to those sections we will calculate the effective diffusion for the case of infinite parallel plates.

We assume that the plates are a distance H_0 apart and that the average velocity between the plates is $\overline{U}^{pp}$. The well known solution for flow between parallel plates shows that the

velocity profile is given by

$$u^{pp}(y) = \overline{U}^{pp} f^{pp}(y/H_0),$$

where

$$f^{pp}(\eta) = 6\left(1/4 - \eta^2\right). \tag{10}$$

In this case we get

$$\sigma_1^{pp} = -\overline{U}^{pp}.$$

The first order term ϕ_1^{pp} in the eigenfunction satisfies

$$D\frac{\mathrm{d}^2\phi_1^{pp}}{\mathrm{d}y^2} = u^{pp}(y) - \overline{U}^{pp},$$
$$\frac{\mathrm{d}\phi_1^{pp}}{\mathrm{d}y} = 0 \text{ at } y = \pm H_0/2.$$

This has the solution

$$\phi_1^{pp}(y) = Pe\ H_0 G^{pp}(y/H_0),$$

where

$$G^{pp}(\eta) = \frac{\eta^2}{4} - \frac{\eta^4}{2} - \frac{7}{480}, \tag{11}$$

and

$$Pe = \frac{\overline{U}^{pp} H_0}{D}.$$

In order to evaluate σ_2 using (8) we are more concerned with the quantity

$$\frac{\mathrm{d}\phi_1^{pp}}{\mathrm{d}y} = Pe\ g^{pp}(y/H_0), \tag{12}$$

where

$$g^{pp}(\eta) = \frac{\mathrm{d}G^{pp}}{\mathrm{d}\eta}. \tag{13}$$

Substituting this solution into (8) we find

$$\sigma_2^{pp} = -D\left(1 + \frac{1}{210}Pe^2\right). \tag{14}$$

Using our definition of K in (1), we see that

$$K^{pp} = \frac{1}{210} \tag{15}$$

4 The Average Velocity in High Aspect Ratio Cross Sections

In order to compute the effective diffusion coefficient it is necessary to compute the average velocity in the column. Although the average velocity in a high aspect ratio cross section is nearly equal to the average velocity between two parallel plates, we will see in § 6 that this small discrepancy can lead to an order one change in the effective diffusion coefficient.

We limit the results of this section to the case where the height away from the ends of the cross section is constant. In § 7 we extend this to the case where the height in the middle of the cross section changes by a small and slowly varying amount.

As in the previous section, $\overline{U}^{pp}$ will denote the average value of the velocity in the parallel plate approximation. If $\overline{u}$ is the true average value of the velocity, we can write

$$\overline{u} = \frac{1}{A}\int_\Omega u \, \mathrm{d}A = \frac{1}{A}\int_\Omega (u - \overline{U}^{pp}) \, \mathrm{d}A + \overline{U}^{pp}. \tag{16}$$

The velocity profile for Poiseuille flow through a rectangular cross section can be written down in terms of an infinite series. This solution shows that for a cross section of height H_0 and width W that has a large aspect ratio ($H_0/W \ll 1$), the velocity approaches the parallel plate profile exponentially fast as we move away from the ends. Significant differences between the parallel plate and true velocity profiles only exist in a region that is on the order of H_0 near the ends. For a channel where the ends are not perfectly straight, we see similar behavior, namely an exponentially fast approach to the parallel plate approximation as we move away from the ends.

Since the velocity is exponentially approaching the parallel plate profile, to a very good approximation, we do not need to compute the integral of $u - \overline{U}^{pp}$ except near the ends. In order to compute this integral near the ends we can isolate each end region. To simplify the explanation we show how to do this for a rectangular cross section, and then note how the results are easily generalized to cross sections that are not rectangular.

For a rectangular cross section, we can analyze the end region by considering the semi-infinite region Ω_L defined by

$$(x, y) \in \Omega_L \text{ iff } x \geq -W/2 \text{ and } \mid y \mid \leq H_0/2.$$

In this end region we consider the problem

$$\begin{aligned} \mu\nabla^2 u &= \frac{\partial p}{\partial z} \text{ in } \Omega_L, \\ u &= 0 \text{ on } \partial\Omega_L, \\ u \to u^{pp}(y) &= \overline{U}^{pp} f^{pp}(y/H_0) \text{ as } x \to \infty. \end{aligned}$$

In order to compute the average velocity we need to compute the integral

$$I_L = \int_{\Omega_L} (u - \overline{U}^{pp}) \, \mathrm{d}A = \int_{\Omega_L} v \, \mathrm{d}A + \int_{\Omega_L} \left(u^{pp}(y) - \overline{U}^{pp}\right) \, \mathrm{d}A, \tag{17}$$

where

$$v = u - u^{pp}(y). \tag{18}$$

Since both u and $u^{pp}(y)$ satisfy the Poisson equation with the same constant right hand side, and u vanishes on the boundary, we have

$$\nabla^2 v = 0, \tag{19a}$$

$$v = -u^{pp}(y) \text{ on } \partial\Omega_L \ , \tag{19b}$$

$$v \to 0 \text{ as } x \to \infty. \tag{19c}$$

If we set

$$v(x, y) = \overline{U}^{pp} \hat{v}(X, Y)$$

where

$$(X, Y) = (x + W/2, y)/H_0,$$

then we have

$$\nabla^2 \hat{v} = 0, \tag{20a}$$

$$\hat{v} = -f^{pp}(Y) = 0 \text{ for } X \geq 0 \text{ and } Y = \pm 1/2, \tag{20b}$$

$$\hat{v} = -f^{pp}(Y) \text{ for } X = 0 \text{ and } \mid Y \mid < 1/2\ , \tag{20c}$$

$$\hat{v} \to 0 \text{ as } X \to \infty. \tag{20d}$$

In terms of these dimensionless variables we can write

$$I_L = -H_0^2 \overline{U}^{pp} \alpha_L, \tag{21}$$

where

$$\alpha_L = -\int_{-1/2}^{1/2} \int_0^\infty \hat{v}(X, Y)\, \mathrm{d}X\, \mathrm{d}Y = -\int_{-1/2}^{1/2} \int_0^\infty \left(f^{pp}(y) - 1\right)\, \mathrm{d}X\, \mathrm{d}Y.$$

The constant α_L is clearly dimensionless.

The computation of α_L for a rectangular cross section can be found in several locations including [13] where it is shown that

$$\alpha_L \approx \frac{96}{\pi^5} \sum_{k=0}^{\infty} \frac{1}{(2k+1)^5} \approx .3151$$

Almost identical arguments would apply if the cross section were not rectangular, but for example had a semi-circular section attached at $x = -W/2$. In this case the region Ω_L would be a region that properly gives the geometry of the end near $x = -W/2$, but ignores the right end, replacing it with a semi-infinite region of constant thickness. In the general case (17), (19), and (21) still hold.

A similar analysis holds when we consider the velocity profile on the right side of the cross section. It follows that our expression for the average velocity can be written as

$$\overline{u} = \overline{U}^{pp} - \frac{\overline{U}^{pp} H_0^2}{A} \left(\alpha_L + \alpha_R\right).$$

Note that $A \approx H_0 W$, so that to first order in ϵ we have

$$\overline{u} = \overline{U}^{pp} - \epsilon \overline{U}^{pp} \left(\alpha_L + \alpha_R\right). \tag{22}$$

5 A Necessary Condition for the Vanishing of α_L

In this section we will show that in order to have α_L vanish, it is necessary that the left end bulges out as in figure 2(a). That is, it is necessary to have $\mid y \mid > H_0/2$ somewhere in the end section. Identical results apply for α_R. A modification of this type to increase the fluid velocity in the end regions was proposed in [10] and was shown to reduce the dispersion. We extend the results of [10] by proving below that such a modification is, in fact, a necessary condition.

Using the expression $u^{pp}(y) = \overline{U}^{pp} f^{pp}(y)$ where $f^{pp}(y)$ is defined in (10), we can show that

$$\frac{1}{2}\left(\frac{1}{12} \mid \nabla u^{pp} \mid^2 - \overline{U}^{pp}\right) + \left(u^{pp} - \overline{U}^{pp}\right) = 0. \tag{23}$$

Using the fact that $\nabla^2 u^{pp} = -12$, and $\nabla^2 v = 0$, we can write (17) for I_L as

$$I_L = \frac{1}{12}\int_{\Omega_L}\left(u^{pp}\nabla^2 v - v\nabla^2 u^{pp}\right)\,\mathrm{d}A + \int_{\Omega_L}\left(u^{pp} - \overline{U}^{pp}\right)\,\mathrm{d}A.$$

Using Green's identity, this gives us

$$I_L = \frac{1}{12}\int_{\partial\Omega_L}\left(u^{pp}\frac{\partial v}{\partial n} - v\frac{\partial u^{pp}}{\partial n}\right)\,\mathrm{d}A + \int_{\Omega_L}\left(u^{pp} - \overline{U}^{pp}\right)\,\mathrm{d}A.$$

We now use the fact that u vanishes on the boundary, and hence $v = -u^{pp}$ on the boundary. This allows us to write

$$I_L = \frac{1}{12}\int_{\partial\Omega_L}\left(u^{pp}\frac{\partial u^{pp}}{\partial n} - v\frac{\partial v}{\partial n}\right)\,\mathrm{d}A + \int_{\Omega_L}\left(u^{pp} - \overline{U}^{pp}\right)\,\mathrm{d}A.$$

Using Green's identity, we can write

$$\int_{\partial\Omega_L} v\frac{\partial v}{\partial n}\,\mathrm{d}S = \int_{\Omega_L} \mid \nabla v \mid^2\,\mathrm{d}A,$$

$$\int_{\partial\Omega_L} u^{pp}\frac{\partial u^{pp}}{\partial n}\,\mathrm{d}S = \int_{\Omega_L}\left(\mid \nabla u^{pp} \mid^2 + u^{pp}\nabla^2 u^{pp}\right)\,\mathrm{d}A = \int_{\Omega_L}\left(\mid \nabla u^{pp} \mid^2 - 12u^{pp}\right)\,\mathrm{d}A$$

It follows that we can write

$$I_L = -\frac{1}{12}\int_{\Omega_L} \mid \nabla v \mid^2\,\mathrm{d}A + \int_{\Omega_L}\left(\frac{1}{12} \mid \nabla u^{pp} \mid^2 - \overline{U}^{pp}\right)\,\mathrm{d}A. \tag{24}$$

If we divide (24) by two, and add the result to (17), and use (23), we get

$$\frac{3}{2}I_L = -\frac{1}{24}\int_{\Omega_L} \mid \nabla v \mid^2 dA + \int_{\Omega_L} v\,\mathrm{d}A. \tag{25}$$

We now use the fact that $u^{pp}(y) > 0$, if $\mid y \mid < H_0/2$. That is, the function giving the parallel plate velocity is always bigger than zero if we evaluate it between the parallel plates. Our boundary condition for v in (19) shows that if we always have $\mid y \mid < H_0/2$, then v is always negative on the boundary. The maximum principle for Laplace's equation now implies that v is always negative. In this case our expression (25) is clearly negative. This shows that if the end does not bulge out, then I_L is negative, and hence α_L is positive.

6 Channels with Mid-Sections of Constant Height

Here we discuss how to compute the effective diffusion coefficient in the case where the cross section is constant away from the ends. We discuss the case where we have a small and slowly varying deviation from a constant cross section in the next section.

We assume that away from the ends $x = \pm W/2$, the cross section has constant height H_0. Near the ends, we can have quite arbitrary shapes. We will assume that $\epsilon \equiv H_0/W \ll 1$. We will also utilize the dimensionless rescalings $\xi = x/W$ and $\eta = y/H_0$.

In order to use (8) to compute σ_2, we need to compute ϕ_1 that satisfies (9), which we write as

$$D\left(\frac{\partial^2\phi_1}{\partial x^2} + \frac{\partial^2\phi_1}{\partial y^2}\right) = u(x,y) - \overline{u} = \left(u(x,y) - \overline{U}^{pp}\right) + \overline{U}^{pp} S(x/W), \tag{26a}$$

where

$$S(\xi) = \frac{\overline{U}^{pp} - \overline{u}}{\overline{U}^{pp}} \approx \epsilon\left(\alpha_L + \alpha_R\right). \tag{26b}$$

In the equation for ϕ_1 we have split the right hand side up into the term $u(x,y) - \overline{U}^{pp}$ whose integral across the slice $x = constant$ vanishes (if we are sufficiently away from the ends), and a source term $S(x/W)$ whose integral across the slice does not vanish. In the case at hand, the function $S(\xi)$ is a constant, but we have chosen to include the functional dependence on ξ since a similar analysis will hold in the next section where $S(\xi)$ will not be a constant.

Away from the ends $x = \pm W/2$ of the cross section, $u(x,y)$ will be very close to Poiseuille flow between parallel plates a distance H_0 apart, Assuming that ϵ is small we expect that the derivatives with respect to x of ϕ_1 will be much smaller than those with respect to y. Furthermore, since $S(\xi)$ is small, we might guess that the leading order term in (26) is given by

$$D\frac{\partial^2\phi_1}{\partial y^2} = U^{pp}(y) - \overline{U}^{pp},$$

along with the boundary conditions $\frac{\partial\phi_1}{\partial y} = 0$ at $y = \pm H_0/2$. This has the solution

$$\phi_1(x,y) = \phi_1^{pp}(y) + F(x), \tag{27a}$$

where

$$\phi_1^{pp}(y) = Pe\ H_0 G^{pp}(y/H_0), \tag{27b}$$

and $G^{pp}(\eta)$ is defined in (11).

Our paradoxical behavior arises from the fact that the function $F(x)$ in (27a) is $1/\epsilon$ larger than the term ϕ_1^{pp}. This is related to the general high aspect ratio case [7] where the leading order term is proportional to $1/\epsilon^2$. The necessity for having a leading order term of $1/\epsilon$ can be seen when trying to compute the next order correction to this term (see Appendix A). Intuitively it arises from the fact that if we include the source $S(x/W)$ in (26), then we cannot solve this equation if we ignore the partial derivatives with respect to x on the left hand side of this equation. The more rigorous perturbation theory shows that the leading order term $F(x)$ must be chosen so that the derivatives on the left cancel the source term $\overline{U}^{pp} S(x/W)$ on the right. That is,

$$DF'' = \overline{U}^{pp} S(x/W). \tag{28}$$

This has the solution

$$F'(x) = \frac{\overline{U}^{pp}}{D}\left(\int_{-W/2}^{x} S(x/W)\,\mathrm{d}x + H_0 C_{int}\right), \tag{29}$$

which can be written as

$$F'(x) = Pe\ \beta(x/W), \tag{30a}$$

where

$$\beta(x/W) = \frac{1}{\epsilon}\left(\int_{-1/2}^{x/W} S(\xi)\,\mathrm{d}\xi + \epsilon C_{int}\right). \tag{30b}$$

At this point the constant C_{int} is not known, but we now show that

$$C_{int} = -\alpha_L. \tag{30c}$$

To do this we define the regions $\Omega(s)$ to be the part of our cross section that has $x \leq s$. If we integrate the equation

$$D\nabla_2^2\phi_1 = u(x,y) - \overline{u}$$

over the region $\Omega(x)$, and use the fact that $\frac{\partial\phi_1}{\partial n}$ vanishes on the boundary of Ω, we get

$$D\int_{x=const} \frac{\partial\phi_1}{\partial x}\,\mathrm{d}y = \int_{\Omega(x)} (u-\overline{u})\;\mathrm{d}x\,\mathrm{d}y.$$

When x is in the interior of the cross section, (27a) shows that the left hand side of this expression is clearly approaching $DH_0F'(x)$. It follows that in the interior of the cross section we have

$$DH_0F'(x) \approx \int_{\Omega(x)} \left(u - \overline{U}^{pp}\right)\;\mathrm{d}x\,\mathrm{d}y + \int_{\Omega(x)} \left(\overline{U}^{pp} - \overline{u}\right)\;\mathrm{d}x\,\mathrm{d}y. \tag{31}$$

Since u is asymptotically approaching $\overline{U}^{pp}$ as x moves away from the end region, the first integral on the right is well approximated by

$$\int_{\Omega(x)} \left(u - \overline{U}^{pp}\right)\;\mathrm{d}x\,\mathrm{d}y \approx -\alpha_L\overline{U}^{pp}H_0^2. \tag{32}$$

The second integral can be approximated by

$$\int_{\Omega(x)} \left(\overline{U}^{pp} - \overline{u}\right)\;\mathrm{d}x\,\mathrm{d}y \approx H_0\overline{U}^{pp}\int_{-W/2}^{x} S(x/W)\,\mathrm{d}x. \tag{33}$$

Note that in making this approximation we have assumed that the height of the channel is everywhere given by H_0, which is not true in the end region, but ignoring this fact gives us an error that is on the order of ϵ. Combining (31), (32), and (33) we see that in the interior we have

$$F'(x) \approx -Pe\;\alpha_L + \frac{Pe}{\epsilon}\int_{-1/2}^{x/W} S(\xi)\,\mathrm{d}\xi.$$

If we compare this to equation (30c), we see that we must have $C_{int} = -\alpha_L$ in order to have these two expressions agree. Now that we know that $C_{int} = -\alpha_L$, we can compute $\beta(x/W)$:

$$\beta(\xi) = (\alpha_L + \alpha_R)\left(\xi + \frac{1}{2}\right) - \alpha_L. \tag{34}$$

We now argue that when computing the integral (8), there is a small contribution to the integral coming from the end regions, but the main contribution comes from the interior region. From (26), we see that the function ϕ_1 in the end region is on the order of $\phi_1 = \mathcal{O}(Pe\;H_0)$. The square of the gradient in the end region will be on the order of $\mid\nabla\phi_1\mid^2 = \mathcal{O}(Pe^2)$. The integral of the square of the gradient in the end region will be on the order of $Pe^2H_0^2$. We will now see that the integral of $\mid\nabla\phi_1\mid^2$ in the interior is on the order of $Pe^2\;H_0W$, which is $1/\epsilon$ bigger than the integral in the end region.

Equations (27a) and (30a) show that in the interior we have

$$| \nabla\phi_1 |^2 \approx Pe^2 \left((g^{pp}(y/H_0))^2 + (\beta(x/W))^2 \right).$$

This term is on the order of Pe^2, so when we integrate it over the whole cross section, we get a term that is on the order of $Pe^2 H_0 W$, which is what we claimed in the last paragraph. Using this form to compute the integral in (8) we get

$$\sigma_2 = -D\left(1 + Pe^2 K\right),$$

where

$$K \approx \frac{1}{210} + \Lambda, \tag{35a}$$

$$\Lambda = \int_{-1/2}^{1/2} \beta^2(\xi)\, \mathrm{d}\xi = \frac{\alpha_L^2 - \alpha_L\alpha_R + \alpha_R^2}{3}. \tag{35b}$$

We emphasize that the effect of the ends gives an order one contribution to the effective diffusion coefficient, even in the limit as $\epsilon \to 0$.

7 Slowly Varying Mid-sections

In this section we extend the results of the last section to include cross sections that have slowly varying mid-sections. The analysis is almost identical to the one in the last section, requiring only that we use a different function $S(\xi)$ for the source term in equation (30c).

We assume that away from the ends, the height of the channel varies like

$$H(x) = H_0\left(1 + \delta\gamma(x/W)\right), \tag{36}$$

where $| \delta | \ll 1$. We also assume that away from the ends $\xi = \pm 1/2$, $\gamma(\xi)$ and its derivative are both order one or less, and that $\epsilon = H_0/W \ll 1$. In other words, we have a nearly rectangular channel that has a small and slowly varying deviation from a rectangular shape in the middle of the cross section, and possibly a large deviation near the ends (for example, semi-circular ends).

In this case, the function ϕ_1 satisfies

$$D\left(\frac{\partial^2\phi_1}{\partial x^2} + \frac{\partial^2\phi_1}{\partial y^2}\right) = u(x,y) - \overline{u} = \left(u(x,y) - \overline{U}(x)\right) + U_0 S(x/W), \tag{37a}$$

where

$$S(x/W) = \frac{\overline{U}(x) - \overline{u}}{\overline{U}^{pp}}. \tag{37b}$$

$\overline{U}(x)$ denotes the average value of the velocity across the slice of the cross section with x held constant:

$$\overline{U}(x) = \int_{x=const} u(x,y)\, \mathrm{d}y. \tag{37c}$$

In the last section $\overline{U}(x)$ was equal to $\overline{U}^{pp}$, but in this section it will vary slowly in the channel.

We need the formula for $S(\xi)$ in the middle of the channel. To derive this we use the fact that the velocity profile for flow between parallel plates a distance h apart is given by

$$u(y) = -\frac{\partial p}{\partial z}\frac{1}{2\mu}(h^2/4 - y^2).$$

Integrating this expression from $y = -h/2$ to $y = h/2$ shows that for a given value of the pressure gradient, the average velocity is proportional to the square of the distance between the plates. In our channel where the thickness varies slowly with x, the average velocity across the slice of the channel with x constant will be very nearly

$$U^{pp}(x) = \frac{H^2(x)}{H_0^2}\overline{U}^{pp} = \overline{U}^{pp}\left(1 + \delta\gamma(x/W)\right)^2.$$

Here $\overline{U}^{pp}$ is the average velocity in plane Poiseuille flow where the plates are a distance H_0 apart, and the pressure gradient is the pressure gradient that is being imposed on our system. Assuming that δ is small we have

$$U^{pp}(x) \approx \overline{U}^{pp} + 2\delta\overline{U}^{pp}\gamma(x/W). \tag{38}$$

In order to compute $S(\xi)$ we need to calculate the average velocity in the channel. In what follows, we will assume that the function $\gamma(\xi)$ is defined so that it properly gives the behavior in the interior of the channel, but makes no attempt to model the profile in the end regions. For example, if we had a rectangular channel that varies linearly in x in the interior region, but has semi-circular end regions; we do not attempt to have the function $\gamma(\xi)$ capture the behavior in the end regions. For this reason, we assume that $\delta\gamma(\xi)$ is small on the whole interval $|\,\xi\,| \leq 1/2$. Although it does not capture the behavior in the end region, we assume that it is still defined in that region.

We can write

$$\overline{u} - \overline{U}^{pp} = \frac{1}{A}\int_\Omega \left(u(x,y) - \overline{U}^{pp}\right)\,\mathrm{d}x\,\mathrm{d}y = \frac{1}{A}\left(I_1 + I_2\right),$$

where

$$I_1 = \int_\Omega \left(u(x,y) - U^{pp}(x)\right)\,\mathrm{d}x\,\mathrm{d}y,$$
$$I_2 = \int_\Omega \left(U^{pp}(x) - \overline{U}^{pp}\right)\,\mathrm{d}x\,\mathrm{d}y.$$

The first of these integrals can be evaluated just as we did in § 4. In particular, we assume that the integrand goes to zero exponentially fast as we move away from the ends. We only need to compute the integral in the end regions. Doing this we get

$$I_1 = -H_0^2\overline{U}^{pp}\left(\alpha_L + \alpha_R\right),$$

where α_L and α_R would be the same constants we would get when the channel asymptotes to a channel of constant height H_0. In doing this we are ignoring terms that are on the order of $\delta H_0^2\overline{U}^{pp}$.

The integral I_2 can be computed by noting that away from the end regions we have

$$\int_{x=constant}\left(U^{pp}(x) - \overline{U}^{pp}\right)\,\mathrm{d}y \approx \overline{U}^{pp}H_0 2\delta\gamma(x/W).$$

This expression is not quite right in the end regions, but when computing I_2, the contribution from the end regions is small, so to a very good approximation we have

$$I_2 \approx \overline{U}^{pp} H_0 \int_{-W/2}^{W/2} 2\delta\gamma(x/W)\,\mathrm{d}x = 2\delta\overline{U}^{pp} H_0 W C_\gamma,$$

where

$$C_\gamma = \int_{-1/2}^{1/2} \gamma(\xi)\,\mathrm{d}\xi. \tag{39}$$

Note that both I_1 and I_2 are small, so when we divide them by A if we make the approximation $A \approx H_0 W$, we get an error that is second order in δ and ϵ. That is,

$$\frac{1}{A}\left(I_1 + I_2\right) \approx -\overline{U}^{pp}\epsilon\left(\alpha_L + \alpha_R\right) + 2\delta\overline{U}^{pp} C_\gamma.$$

This shows us that

$$\frac{\overline{U}^{pp}}{\overline{U}^{pp}} \approx 1 - \epsilon\left(\alpha_l + \alpha_R\right) + 2\delta C_\gamma. \tag{40}$$

Using the definition of $S(\xi)$ in (37b), (38), and the expression in (40), we get

$$S(\xi) \approx 2\delta\gamma(\xi) + \epsilon\left(\alpha_L + \alpha_R\right) - 2\delta C_\gamma \text{ for } x \text{ away from the ends.} \tag{41}$$

As in the previous section, the solution ϕ_1 in the interior can be written as

$$\phi_1(x, y) \approx \overline{U}^{pp} H_0 G^{pp}(y/H_0) + F(x),$$

where F' is given by (29). We can use the same argument as in the last section to show that $C_{int} = -\alpha_L$. This implies that we can write

$$F'(x) = Pe\ \beta(x/W),$$

where

$$\beta(\xi) = \frac{\delta}{\epsilon} B(\xi) + \left(\alpha_L + \alpha_R\right)\left(\xi + \frac{1}{2}\right) - \alpha_L, \tag{42a}$$

and where

$$B(\xi) = 2\int_{-1/2}^{\xi} \gamma(s)\,\mathrm{d}s - 2(\xi + 1/2)C_\gamma. \tag{42b}$$

As in the last section we have

$$\sigma_2 = \sigma_2^{pp} - Pe^2\Lambda, \tag{43a}$$

where

$$\Lambda = \int_{-1/2}^{1/2} \beta^2(s)\,\mathrm{d}s, \tag{43b}$$

and σ_2^{pp} is given in (14). Our expression for σ_2 implies that

$$K = K^{pp} + \Lambda \tag{44}$$

We illustrate this formula with two examples. Suppose that we have a symmetric channel with a quadratic variation in height. In this case we have $\gamma(\xi) = \xi^2$, and $\alpha_L = \alpha_R = \alpha$. Substituting these expressions into (43b) we get

$$\Lambda = Pe^2 \frac{630\alpha^2 - 42\alpha\delta/\epsilon + \delta^2/\epsilon^2}{1890}. \tag{45}$$

If we set $\delta = 0$, we get the result

$$\Lambda = Pe^2 \frac{\alpha^2}{3}.$$

We can minimize this expression by setting $\delta/\epsilon = 21\alpha$. If we do this we get

$$\Lambda = Pe^2 \frac{\alpha^2}{10}.$$

In order to facilitate comparison between our results and those in [12] we give the example $\gamma(\xi) = 4\xi^2 - 1$ that is used in that paper. Assuming that $\alpha_L = \alpha_R = \alpha$, we get

$$\Lambda = \frac{\alpha^2}{3} - \frac{4\alpha\delta}{45\epsilon} + \frac{8\delta^2}{945\epsilon^2}$$

This agrees with equation 29 in [12]. (We note that α, δ, and $K = K^{pp} + \Lambda$ here are called, respectively, δ, ϵ, and $f/210$ in [12]).

As another example, we suppose that we have a linear variation in the height of the cross section. This gives us

$$\Lambda = Pe^2 \left(\frac{\alpha^2}{3} + \frac{\delta^2}{30\epsilon^2} \right). \tag{46}$$

8 Numerical Results

In this section, we first numerically confirm the effective diffusion coefficients for the high aspect ratio models developed in the previous section. We then explore a modification of the ends of a channel of rectangular cross section that minimizes the end effects discussed in § 6. Finally, we numerically minimize σ_2 for a cross section with asymmetric ends.

8.1 Model Confirmation

In this section we confirm via numerical experiment the expressions in (45) and (46).

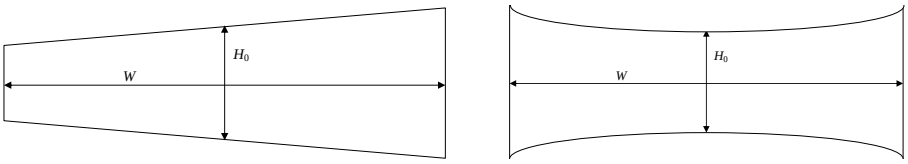

(a) Linear side walls. (b) Quadratic side walls.

Fig. 1. Cross sections of nearly rectangular columns with height H_0 and width W.

We first consider a model with linear side walls. Let the height be described in (36), with $\gamma(\xi) = \xi$, and $\delta = 0.05$. The correction to the effective diffusion of the parallel plate case is given by (46). An example cross section is shown in figure 1(a). We fix the height $H_0 = 1$ and numerically compute the velocity profile for various values of W, fixing the Péclet number to be $Pe = 1$. We then determine the eigenvalue $\sigma(k)$ for several values of k, and do a polynomial fit of $\sigma(k)$ to determine σ_1 and σ_2. Theoretical values of Λ from (46) are compared with

Aspect Ratio	σ_2	Numerical Λ	Theoretical Λ	Relative Error
1	1.0084	-0.0295	0.0000	354.7987
10	1.0451	0.0072	0.0083	0.1355
20	1.0695	0.0316	0.0333	0.0507
40	1.1569	0.1191	0.1333	0.1069
80	1.5422	0.5043	0.5333	0.0544
160	3.1154	2.0775	2.1333	0.0262
320	9.6658	8.6280	8.5333	0.0111

Table 1
Numerically determined values of σ_2 for various aspect ratios for a cross-section with linear side walls. The numerical correction value is compared with the theoretical correction value Λ from equation (46).

Aspect Ratio	σ_2	Numerical Λ	Theoretical Λ	Relative Error
1	1.0086	-0.0293	-0.0007	41.1190
10	1.0291	-0.0088	-0.0065	0.3574
20	1.0261	-0.0118	-0.0119	0.0116
40	1.0191	-0.0188	-0.0195	0.0376
80	1.0154	-0.0225	-0.0222	0.0135
160	1.0571	0.0192	0.0234	0.1785
320	1.3428	0.3050	0.3177	0.0401

Table 2
Numerically determined values of σ_2 for various aspect ratios for a cross-section with quadratic side walls. The numerical correction value is compared with the theoretical correction value Λ from equation (45).

numerical values of Λ in table 1, and the relative error tabulated. Note that the theoretical results are valid only in the case of a large aspect ratio.

Of interest in this model is that σ_2 approaches infinity with W, whereas a column with a perfectly rectangular cross section (corresponding to $\delta = 0$) has σ_2 approaching a value close to one. This rapid growth in σ_2 is confirmed numerically in table 1.

We next consider a model with quadratic side walls. In this case, $\gamma(\xi) = \xi^2$, and the correction to the effective diffusion of the parallel plate case is given in (45). An example cross section is shown in figure 1(b). We have again chosen $\delta = 0.05$, and fixed $Pe = 1$ and $H_0 = 1$. Following the same procedure as before, we numerically compute the velocity profile for various values of W. We then determine the eigenvalue $\sigma(k)$ for several values of k, and then do a polynomial fit of $\sigma(k)$ to determine σ_1 and σ_2. Theoretical values of Λ from (45) are compared with numerical values of Λ in table 2, and the relative error tabulated. Again, note that the theoretical results are valid only in the case of a large aspect ratio.

Of interest in this model is that σ_2 again approaches infinity with W, but does so much less slowly than for the linear model. This reduced growth in σ_2 is confirmed numerically

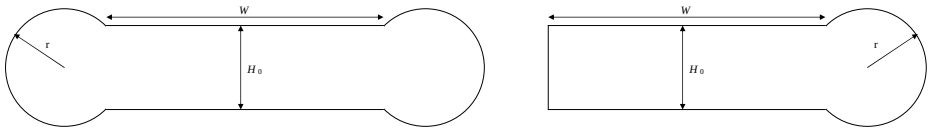

(a) Symmetric ends. (b) Asymmetric ends.

Fig. 2. Cross sections of nearly rectangular columns with height H_0 and width W with with one or two bulb shaped ends of radius r.

in table 2. Also note that from (45), there is a sign change in the correction term, meaning that for a particular aspect ratio, the expected value of σ_2 is the same as for a perfectly rectangular cross section. This change of sign is observed in table 2. As we would expect, there is an increase in the relative error near this critical point, although the absolute error remains quite small.

8.2 Minimization of End Effects

In this section, we consider modifying the ends of a channel of rectangular cross section to minimize the effects discussed in § 6. In particular, we seek an end configuration such that Λ in (35) is essentially zero.

Following a hint given in [6], we consider using a "bulb" on the ends of the channel cross section, as shown in figure 2(a). We set the height $H_0 = 1$ and the width $W = 100$. For a circular bulb of radius $r = 0.7$, we numerically observe that the term Λ in (35) is 0.00039. In effect, this high aspect ratio channel has the effective diffusion coefficient of two parallel plates, and the effect of the ends has been removed.

8.3 Asymmetric Ends

Here we consider a cross section similar to that in figure 2(a), but with the right end a bulb of radius r and the left end rectangular. We set the height $H_0 = 1$ and the width $W = 100$. We seek to minimize σ_2 by varying the radius r, which means minimizing Λ in (35). § 5 tells us that since the left end of the cross section does not bulge out like the right end, we can never eliminate the end effects (i.e., make $\Lambda = 0$). Numerically determined values of σ_2 are shown in table 3 as a function of r. We see that the smallest observed value of σ_2 occurred for $r = 0.63$.

Acknowledgements

The authors wish to acknowledge many helpful discussions with Joshua Whiting and Robert Simonson of the Micro Analytical Systems department at Sandia National Laboratories. Additionally, the authors would like to thank Prof. David Leighton of the department of chemical and biomolecular engineering at the University of Notre Dame for answering questions about his papers and identifying the correction to equation 14 of [12]. The authors would also like to acknowledge Pavel Bochev of the Computational Mathematics and Algorithms department at Sandia National Laboratories.

r	σ_2
0.61	1.0298
0.62	1.0295
0.63	**1.0293**
0.64	1.0294
0.65	1.0298
0.66	1.0305

Table 3
Numerically determined values of σ_2 for various values of the radius r for a cross section with asymmetric ends. The minimum value of σ_2 observed occurred for $r = 0.63$.

References

[1] P.C. Chatwin and P.J. Sullivan. The effect of aspect ratio on longitudinal diffusivity in rectangular channels. *J. Fluid Mech.*, 120:347–358, July 1982.

[2] M.R. Doshi, P.M. Daiyai, and W.N. Gill. Three dimensional laminar dispersion in open and closed rectangular conduits. *Chem. Eng. Sci.*, 33:795–804, 1978.

[3] G.I. Taylor. Dispersion of soluble matter in solvent flowing slowly through a tube. *Proc. Roy. Soc. Lond. A*, 219(1137):186–203, August 1953.

[4] R. Aris. On the dispersion of a solute in a fluid flowing through a tube. *Proc. Roy. Soc. Lond. A*, 235:67–77, 1956.

[5] M.J.E. Golay. Theory of chromatography in open and coated tubular columns with round and rectangular cross-sections. In D. H. Desty, editor, *Gas Chromatography 1958*, pages 36–53. Butterworths Publications LTD., 1958.

[6] M.J.E. Golay. The height equivalent to a theoretical plate of retentionless rectangular tubes. *J. Chromotography*, 216:1–8, 1981.

[7] D.C. Guelle, R.G. Cox, and H. Brenner. Taylor dispersion in conduits of large aspect ratio. *Chem. Eng. Comm.*, 58:231–244, 1987.

[8] H. Brenner and D.A. Edwards. *Macroscopic Processes*. Butterworth-Heinemann, Boston, Ma, 1993.

[9] A. Ajdari, N. Bontoux, and H. Stone. Hydrodynamic dispersion in shallow microchannels: the effect of cross-sectional shape. *J. Anal. Chem.*, 78:387–392, 2006.

[10] D. Dutta and D.T. Leighton Jr. Dispersion reduction in pressure-driven flow through microetched channels. *J. Anal. Chem.*, 73:504–513, 2001.

[11] D. Dutta and D.T. Leighton Jr. Dispersion in large aspect ratio microchannels for open channel liquid chromatography. *J. Anal. Chem.*, 75:57–70, 2003.

[12] D. Dutta, A. Ramachandran, and D.T. Leighton Jr. Effect of channel geometry on solute dispersion in pressure-driven microfulidic systems. *Microfluid Nanofluid*, 2:275–290, 2006.

[13] G. Desmet and G.V. Baron. Chromatographic explanation for the side-wall induced band broadening in pressure-driven and shear-driven flows through channels with a high aspect-ratio rectangular cross-section. *J. Chromatography A.*, 946:51–58, 2002.

[14] M. Pagitsas, A. Nadim, and H. Brenner. Multiple time scale analysis of macrotransport processes. *Physica*, 135A:533–550, 1986.

[15] R. Mauri and S. Haber. Time-dependent dispersion of small particles in rectangular conduits. *SIAM J. Appl. Math*, 51(6):1538–1555, 1991.

[16] A. Cifuentes and H. Poppe. Rectangular capillary elecrophoresis: Some theoretical considerations. *Chromatographia*, 39(6):391–404, 1994.

[17] A.N. Stokes and N.G. Barton. The concentration distribution produced by shear dispersion of solute in Poiseuille flow. *J. Fluid Mech.*, 210:201–221, 1990.

[18] V. Balakotaiah and H.-C. Chang. Dispersion of chemical solutes in chromatographs and reactors. *Phil. Trans. R. Soc. Lond A*, 351:39–75, 1995.

[19] M. Latini and A.J. Bernoff. Transient anomalous diffusion in Poiseuille flow. *J. Fluid Mech.*, 441:399–411, 2001.

Appendix A

The purpose of this appendix is to give a more rigorous justification of the fact that the function $F(x)$ must satisfy (28) in the interior region of the cross section. To simplify the discussion, we consider the case where $\delta = 0$; a similar discussion holds for $\delta \neq 0$.

To do this we define the dimensionless variables

$$\xi = x/W, \qquad \eta = y/H_0, \qquad \psi = \phi_1/H_0.$$

In the interior region, the velocity is very nearly equal to the parallel plate velocity $u^{pp}(y)$. In terms of the dimensionless variables, the equation for ϕ_1 in the interior can be written as

$$\left(\epsilon^2 \frac{\partial^2 \psi}{\partial \xi^2} + \frac{\partial^2 \psi}{\partial \eta^2}\right) = Pe\ (f^{pp}(\eta) - 1) + Pe\ \epsilon(\alpha_L + \alpha_R),$$

along with the boundary conditions

$$\frac{\partial \psi}{\partial \eta} = 0 \text{ at } \xi = \pm 1/2.$$

We now do a formal perturbation expansion assuming that ϵ is small. In particular we will assume that

$$\psi(\xi, \eta) = \frac{1}{\epsilon}\psi_{-1}(\xi, \eta) + \psi_0(\xi, \eta) + \epsilon\psi_1(\xi, \eta) + \ldots.$$

We have chosen to start the expansion with $1/\epsilon$ because, as we will see, this is necessary in order to satisfy the equations.

If we collect powers of $1/\epsilon$, we see that we must have

$$\frac{\partial^2 \psi_{-1}}{\partial \eta^2} = 0,$$
$$\frac{\partial \psi_{-1}}{\partial \eta} = 0 \text{ at } \eta = \pm 1/2.$$

This implies that we have

$$\psi_{-1}(\xi, \eta) = F(\xi).$$

As we shall see, the fact that ψ_{-1} is independent of η is in fact the main result of this appendix.

If we now carry out the expansion to zeroth order, we find that

$$\frac{\partial^2 \psi_0}{\partial \eta^2} = Pe\ (f^{pp}(\eta) - 1),$$
$$\frac{\partial \psi_0}{\partial \eta} = 0 \text{ at } \eta = \pm 1/2.$$

This implies that

$$\psi_0(\xi, \eta) = Pe\ G^{pp}(\eta) + F(\xi).$$

Finally collecting the powers of ϵ, we find that

$$\frac{\mathrm{d}^2 F}{\mathrm{d}\xi^2} + \frac{\partial^2 \psi_1}{\partial \eta^2} = Pe\ (\alpha_L + \alpha_R),$$
$$\frac{\partial \psi_1}{\partial \eta} = 0 \text{ at } \eta = \pm 1/2.$$

In order to be able to solve for ψ_1 we must satisfy the compatibility condition

$$\int_{-1/2}^{1/2} \left(\frac{\mathrm{d}^2 F}{\mathrm{d}\xi^2} - Pe\ (\alpha_L + \alpha_R) \right) \mathrm{d}\eta = 0.$$

This implies that

$$F(\xi) = Pe\ (\alpha_L + \alpha_R) \frac{\xi^2}{2} + A_1 \xi + A_0.$$

We could continue in this fashion, to determine the terms to higher and higher order, but this is sufficient to see that the form we guessed in § 6 is in fact correct. In particular, it is not necessary to know the function $F(\xi)$ in order to compute the limit of the effective diffusion coefficient as $\epsilon \to 0$.

Appendix B

In this appendix we briefly outline how to compare the results in [12] to those in this paper. We first explain the proper relationships between their and our notations. What they call f is related to what we call K by

$$K = \frac{f}{210}.$$

We use $h(x)$ for what they call $h^\star(x)$, $g(x)$ for what they call $g^\star(x)$, ϵ for what they call d/W, $v(x)$ for what they call $\overline{u}^\star$, V for what they call $\overline{U}^\star$, and α for what they call δ. Here we are assuming that $\alpha_L = \alpha_R = \alpha$, as is assumed in their paper. Equation 14 in [12] states

$$\frac{1}{h(x)}\frac{\mathrm{d}}{\mathrm{d}x}\left(h(x)g'(x)\right) = k - \frac{v(x)}{V}, \tag{B1a}$$

$$g'(\pm 1/2) = \mp \alpha k \epsilon, \tag{B1b}$$

$$\int_{-1/2}^{1/2} g(x)h(x)dx = \alpha\epsilon\left(g(-1/2) + g(1/2)\right). \tag{B1c}$$

Readers of [12] may be confused because (B1b) and (B1c) have been incorrectly typeset as a single equation without a separating semicolon. Here the constant k is given by

$$k = \frac{\int_{-1/2}^{1/2} h(x)\,\mathrm{d}x}{2\alpha\epsilon + \int_{-1/2}^{1/2} h(x)\,\mathrm{d}x}$$

The expression for f in equation 15 of [12] is

$$f = \frac{\int_{-1/2}^{1/2}(v(x)/V)^2 h^3(x)\,\mathrm{d}x}{\int_{-1/2}^{1/2} h(x)\,\mathrm{d}x} + 210\frac{1}{\epsilon^2}\frac{\int_{-1/2}^{1/2}\frac{v(x)}{V}g(x)h(x)\,\mathrm{d}x}{\int_{-1/2}^{1/2} h(x)\,\mathrm{d}x} \tag{B2}$$

We can transform this expression for f into an expression that only depends on the derivative of g by using (B1a) to convert the second integral to the integral of $(v(x)/V - k)\,h(x)g(x)$, plus an additional boundary term. We can then use (B1b) to write this as the integral of $-(h(x)g')'g(x)$. After integrating by parts and using the boundary conditions (B1c), we arrive at

$$f = \frac{\int_{-1/2}^{1/2}(v(x)/V)^2 h^3(x)\,\mathrm{d}x}{I_1} + 210\frac{1}{\epsilon^2}\frac{\int_{-1/2}^{1/2} h(x)(g'(x))^2\,\mathrm{d}x}{I_1} \tag{B3}$$

If we now let $h(x) = 1 + \delta\gamma(x)$, and assume that $\delta \ll 1$ (what we call δ they call ϵ), we find that to first order in δ and ϵ, what we call $\beta(x)$ is related to $g(x)$ by

$$\beta(x) = -\frac{g'(x)}{\epsilon}.$$

We now see that our expressions (43b) and (44) agree with (B2) in the limit as δ and ϵ approach zero.